



## Full paper

## Two new *Mycena* section *Calodontes* species: One newly discovered and the other new to Japan

Kosuke Nagamune<sup>a</sup>, Kentaro Hosaka<sup>b</sup>, Shiro Kigawa<sup>c</sup>, Ryo Sugawara<sup>d</sup>, Kozue Sotome<sup>e</sup>, Akira Nakagiri<sup>e</sup>, Naoki Endo<sup>e\*</sup>

<sup>a</sup> Graduate School of Sustainability Science, Tottori University, 4-101 Koyama, Tottori, 680-8550, Japan

<sup>b</sup> Department of Botany, National Museum of Nature and Science, 4-1-1 Amakubo, Tsukuba, Ibaraki, 305-0005, Japan

<sup>c</sup> Magarimatsu 1-11-13, Hadano, Kanagawa, 259-1321, Japan

<sup>d</sup> The United Graduate School of Agricultural Sciences, Tottori University, 4-101, Koyama, Tottori, 680-8553, Japan

<sup>e</sup> Fungus/Mushroom Resource and Research Center, Faculty of Agriculture, Tottori University, 4-101, Koyama, Tottori, 680-8553, Japan

### ABSTRACT

In 2017, two candidate species of *Mycena* were reported from Japan, with the Japanese names “*Togari-sakura-take*” and “*Mitsuhi-da-sakura-take*”. However, to date, no taxonomic study or formal description has been undertaken for these two species. In the present study, we conducted comprehensive morphological and molecular phylogenetic examinations of “*Togari-sakura-take*” and “*Mitsuhi-da-sakura-take*”, and compared them to known species within the genus *Mycena*. We performed phylogenetic analyses on a concatenated dataset, including the internal transcribed spacer region of ribosomal RNA, RNA polymerase II largest subunit, and translation elongation factor-1 alpha genes. “*Togari-sakura-take*” formed a clade with *Mycena subulata*, which was recently described from China, whereas “*Mitsuhi-da-sakura-take*” formed a distinct independent clade. We identified the former as *M. subulata* based on molecular phylogenetic analyses and morphological observations. However, the Japanese specimens displayed dextrinoid cheilocystidia and caulocystidia as well as the inamyloidity of basidiospores, which differed from the original description of *M. subulata* based on the materials from China. “*Mitsuhi-da-sakura-take*” was characterized by its remarkably dense lamellae and could be distinguished from known *Mycena* species by the combination of absent pleurocystidia and presence of bowling pin-shaped cheilocystidia. Here, we describe “*Mitsuhi-da-sakura-take*” as a new species, named *Mycena densilamellata*, in the section *Calodontes*.

**Keywords:** molecular phylogeny, morphology, *Mycenaceae*, new to Japan, 1 new taxon

**Article history:** Received 25 September 2023, Revised 2 February 2024, Accepted 7 February 2024, Available online 20 May 2024.

### 1. Introduction

The genus *Mycena* (Pers.) Roussel belongs to the family *Mycenaceae* Overeem and order *Agaricales* Underw. (Wijayawardene et al., 2020). This genus is one of the species-rich taxa within *Agaricales*, with approximately 600 valid species, according to the Index Fungorum database (<http://www.indexfungorum.org/>; accessed on Dec 5 2023) and recent studies on the phylum *Basidiomycota* (e.g., He et al., 2019). In Japan, approximately 70 *Mycena* species have been reported to date (Cha et al., 2010; Katumoto, 2010; Shirayama, 2010; Terashima et al., 2016). *Mycena* typically produces small to medium-sized mycenoid, omphalinoid, or collybioid basidioma, and possesses smooth or branched-cheilocystidia and pleurocystidia, diverticulate, and less frequently smooth hyphae of pileipellis. In addition, the lamella trama appears vinaceous to pur-

plish brown (dextrinoid) upon staining with Melzer’s reagent, whereas basidiospores are generally amyloid (Maas Geesteranus, 1980). Similar to other agarics, the taxonomy of *Mycena* is undergoing a transition from conventional research methods relying heavily on the morphological characteristics of basidiomata (Maas Geesteranus, 1980) to approaches focusing more on molecular phylogenetic analyses (Harder et al., 2010; Liu et al., 2022).

*Mycena* species have diverse lifestyles, primarily as saprophytes, while certain species are recognized as orchid mycorrhizal symbionts or plant pathogens (Kitahara et al., 2022; Krishnan, 2017). Some *Mycena* species are known to invade and associate with mosses (Davey et al., 2013). Recent insights into the role of *Mycena* species as symbionts of plants have been provided through the inoculation of cultured strains onto their host plants (Thoen et al., 2020) as well as field observations (Harder et al., 2023). Therefore, further taxonomic studies incorporating ecology are needed to understand the species diversity of the genus *Mycena*.

*Mycena* section *Calodontes* (Fr. ex Berk.) Quél. sensu Maas Geesteranus (1989) generally produces basidioma with raphanoid

\* Corresponding author. Fungus/Mushroom Resource and Research Center, Faculty of Agriculture, Tottori University, 4-101, Koyama, Tottori, 680-8553, Japan  
E-mail address: endo\_nao@tottori-u.ac.jp (N. Endo).



odor and diverse colors (frequently with purplish or violaceous tints), as well as smooth cheilocystidia, pleurocystidia, and smooth hyphae of pileipellis (Maas Geesteranus, 1989). This section is divided into four subsections according to their morphological characteristics (Maas Geesteranus, 1989; Maas Geesteranus & de Meijer, 1997). Subsection *Violacellae* Sing. ex Maas Geest. lectotypified by *M. violacella* (Speg.) Singer [= *Poromyцена violacella* (Speg.) Singer], is unique in having inamyloid basidiospores and lacking pleurocystidia. Subsection *Purae* (Konr. and Maubl) Maas Geest., lectotypified by *M. pura* (Pers.) P. Kumm., is characterized by the presence of amyloid basidiospores, cheilocystidia, and commonly has pleurocystidia with colorless contents. Subsection *Marginatae* J.E. Lange, lectotypified by *M. pelianthina* (Fr.) Quél., also has amyloid basidiospores but is unique among the various validated subsections in forming cheilocystidia and pleurocystidia with purplish brown contents. Subsection *Generosae* Maas Geest. & de Meijer, type species, *M. generosa*, also produces amyloid basidiospores but is distinct as it lacks pleurocystidia and has cheilocystidia with much narrow necks, which are not broadly rounded at the apex.

Harder et al. (2010) attributed almost 30 species to sect. *Calodontes*. Since then, several taxonomic studies from Asia have proposed taxonomic revisions, and around 10 taxa have been added to this section: *M. cahaya* A.L.C. Chew & Desjardin, *M. polycystidiata* Z.W. Liu, Y.P. Ge, L. Zou & Q. Na, *M. rufobrunnea* Z.W. Liu, Y.P. Ge & Q. Na, *M. seminau* A.L.C. Chew & Desjardin, *M. shengshanensis* Z.W. Liu, Y.P. Ge & Q. Na, *M. sinar* A.L.C. Chew & Desjardin, *M. sirayuktha* Aravind. & Manim., *M. subulata* Z.W. Liu, Y.P. Ge & Q. Na, *M. yuezhui* Z.W. Liu, Y.P. Ge & Q. Na, and a new variety *M. sinar* var. *tangkaisinar* A.L.C. Chew & Desjardin (Aravindakshan & Manimohan, 2015; Chew et al., 2014; Liu et al., 2021, 2022). Despite the description of multiple new species from Asia, only four, i.e., *M. pelianthina*, *M. pura*, *M. rosea* Gramberg, and *M. subaquosa* A.H. Sm., have been reported from Japan (Hongo, 1953; Imai, 1938; Kudo & Nagasawa, 2009, 2017; Murata, 1979). Therefore, additional species are expected to be found in Japan.

Kigawa (2017) introduced two *Mycena* species, “*Mycena* sp.”-1 and “*Mycena* sp.”-2, which likely belong to sect. *Calodontes* based on their morphology. Kigawa (2017) suggested that these were new species and gave “*Mycena* spp.”- 1 and 2 the Japanese names of “*Togari-sakura-take*” due to its awl-shaped cheilocystidia and “*Mitsu-hida-sakura-take*” due to its crowded lamellae, respectively. The taxonomic positions of “*Togari-sakura-take*” and “*Mitsu-hida-sakura-take*” are unclear.

The present study evaluated the taxonomic position of “*Togari-sakura-take*” (“*Mycena* sp.”-1) and “*Mitsu-hida-sakura-take*” (“*Mycena* sp.”-2) described by Kigawa (2017) from Japan at the species and subsection levels. To this end, we used the two specimens examined by Kigawa (2017), which are stored at the Hiratsuka

City Museum, and our newly collected specimens from various areas in Japan. We compared the morphology between these two species and other species of the *Mycena* section *Calodontes*. We performed phylogenetic analyses using the DNA sequences of the internal transcribed spacer (ITS) region of ribosomal RNA, RNA polymerase II largest subunit (RPB1), and translation elongation factor-1 alpha (TEF1) genes.

## 2. Materials and methods

### 2.1. Collection of basidiomata specimens and cultures

Each three basidiomata of “*Mycena* spp.”- 1 and 2 were collected from five areas of Japan between Sep and Oct of 2019–2021 (Table 1). Fresh basidiomata were examined macroscopically, air-dried at 45 °C for 1–2 d, and stored. To preserve specimens in a good condition for a long period with a minimum damage, we obtained five cultures that can be used repeatedly for destructive DNA analyses on 1.5% malt extract agar medium containing 1.5% malt extract (Oriental Yeast Co., Ltd., Tokyo, Japan) and 1.5% agar (Fujifilm Wako Pure Chemical Corp., Osaka, Japan) from each fresh basidioma. The dried specimens and cultures were deposited in the Fungus/Mushroom Resource and Research Center (FMRC), Tottori University (Table 1). Fungal strains deposited were cryopreserved in a vapor-phase liquid nitrogen tank at –190 °C. Deposition and utilization of Tottori University Fungal Culture Collection (TUFC) strains were supported by FMRC through the National BioResource Project of the Ministry of Education, Culture, Sports, Science and Technology (MEXT), Japan (<http://nbrp.jp>). We also examined two specimens housed at the fungal herbarium of National Museum of Nature and Science (TNS; TNS-F-75029 and TNS-F-75058) for morphological and phylogenetic analyses. Furthermore, we assessed the morphology of the two specimens examined by Kigawa (2017) that were housed at the Hiratsuka City Museum (HCM-58-6667 and HCM-58-6665) (Table 1).

### 2.2. Morphological observations of basidiomata

The fresh basidiomata in the fields were photographed, and their forest habitats were recorded. The Online Auction Color Chart (Kramer, 2004) was used as the color standard. Microscopic characters of dried specimens were observed in Melzer’s reagent, 3% potassium hydroxide or distilled water using a differential interference contrast microscope (Eclipse 80i, Nikon Co., Tokyo, Japan). The measurements of basidia [not including sterigmata (apical processes for basidiospore production)], basidioles, basidiospores, and cheilocystidia were shown as “(a)b–c(d)”, where (a) indicates the 5th percentile, (b) indicates the average – standard deviation

**Table 1** – *Mycena* specimens examined in this study.

Species	Specimen number in herbarium	Strain number in culture collection	Locality in Japan	Collection date	Vegetation <sup>a</sup>
“ <i>Mycena</i> sp.”-1	TUMH 65483	TUFC 102001	Daisen Town, Tottori Pref.	11 Sep 2021	<i>Fagus crenata</i>
	TUMH 65484	TUFC 102002	Tottori City, Tottori Pref.	19 Sep 2021	<i>Chamaecyparis obtusa</i> , <i>Betula grossa</i> , <i>Acer</i> sp.
	TUMH 65485	TUFC 102003	Kotoura Town, Tottori Pref.	20 Sep 2021	<i>Aesculus turbinata</i> , <i>F. crenata</i> , <i>Acer</i> sp.
	TNS-F-75058		Chichibu City, Saitama Pref.	28 Sep 2015	ND
	HCM-58-6665		Gotenba City, Shizuoka Pref.	13 Sep 2009	ND
“ <i>Mycena</i> sp.”-2	TUMH 65481	TUFC 101999	Ebetsu City, Hokkaido	14 Sep 2019	<i>Picea</i> spp., Betulaceae
	TUMH 65486		Narusawa Village, Yamanashi Pref.	8 Oct 2020	<i>Quercus crispula</i> , <i>F. crenata</i> , <i>C. obtusa</i>
	TUMH 65482	TUFC 102000	Tottori City, Tottori Pref.	19 Sep 2021	<i>C. obtusa</i> , <i>Quercus serrata</i> , <i>Carpinus</i> sp.
	TNS-F-75029		Chichibu City, Saitama Pref.	28 Sep 2015	ND
	HCM-58-6667		Gotenba City, Shizuoka Pref.	13 Sep 2009	ND

<sup>a</sup> ND: No data

(SD), (c) indicates the average + SD, and (d) indicates the 95th percentile. We measured the minimum and maximum values of sterigmata and caulocystidia. The hyphae length/width are shown as 'minimum–maximum'. We measured 50 basidiospores and 30 basidia, basidioles, and cheilocystidia each. Because certain *Mycena* species in sect. *Calodontes* showed a weak amyloid reaction on their basidiospores, we determined the dyeability of basidiospores under differential interference contrast and normal mode light microscopes after treatment with Melzer's reagent for 20 min.  $Q$  and its average value ( $Q_m$ ) were calculated from the length/width ratio of basidiospores. We also observed pileipellis, stiptipellis, and structures of hymenophoral trama.

### 2.3. DNA extraction, PCR amplification, and sequencing

Genomic DNA for PCR amplification was extracted from dried basidioma or living cultures following the method described by Hosaka and Nam (2023) or the microwave method described by Izumitsu et al. (2012). We amplified the full length of the ITS (ITS1–5.8S–ITS2) region and portions of the RPB1 and TEF1 genes. We used Dream Taq DNA Polymerase (Thermo Fisher Scientific, Waltham, MA, USA) for PCR amplification with the following primer pairs: ITS1F and LR5 for ITS region (Gardes & Bruns, 1993; Vilgalys & Hester, 1990), RPB1Mp\_f1 and RPB1Mp\_r1 for RPB1 gene (Harder et al., 2013), and tEFMp\_f1 and tEFMp\_r1 or EF526f/EF595f and EF1567r for TEF1 gene (Harder et al., 2013; Kausarud & Schumacher, 2001; Rehner & Buckley, 2005). PCR was performed using the standard protocol: 35 cycles at 95 °C for 30 s, 49.5 °C for 30 s, and 72 °C for 100 s in the ITS1F and LR5 primer pair; 35 cycles at 95 °C for 30 s, 53 °C for 30 s, and 72 °C for 60 s in the RPB1MP\_f1 and RPB1MP\_r1 primer pair; 35 cycles at 95 °C for 30 s, 52 °C for 30 s, and 72 °C for 60 s in tEFMP\_f1 and tEFMP\_r1 primer pair; 35 cycle of 95 °C for 30 s, 51 °C for 30 s, and 72 °C for 60 s in the EF526f and EF1567r primer pair. For the PCR amplifications of TEF1 gene using the primer pair EF595f and EF1567r, we used touchdown protocols (annealing temperature lowered by 1 °C per cycle), with the following PCR protocol: 35 cycles at 95 °C for 30 s, 60 °C for 30 s, and 72 °C for 60 s. The PCR products were purified using the QIAquick PCR Purification Kit (Qiagen, Hilden, Germany) and directly sequenced using the same pair of bidirectional primers for TEF1 and RPB1 genes or ITS5 and ITS4 primers (White et al., 1990) for the ITS region. The nucleotide sequences were analyzed by FASMAC Co., Ltd. (<http://fasmac.co.jp>), and subsequent phylogenetic analyses of the sequencing data were performed using Bioedit v. 7.2.5 (Hall, 1999). The new sequences were deposited into the GenBank database with accession numbers (LC777686–LC777693, LC777726–LC777741) through the DNA Data Bank of Japan (Table 2).

### 2.4. Phylogenetic analyses

The three loci datasets of ITS, RPB1, and TEF1 were used for phylogenetic analyses. The 64 sequences (Binder et al., 2010; Harder et al., 2013; Liu et al., 2021, 2022) obtained from the National Center for Biotechnology Information GenBank and the eight sequences identified by this study were analyzed (Table 2). From these sequences, we selected *Mycena rubromarginata* (Fr.) P. Kumm. and *M. plumbea* P. Karst. as outgroups (Table 2). *Mycena rubromarginata* was selected as an outgroup due to its previous use in Harder et al. (2013). *Mycena plumbea* occupies the closest position to *M. rubromarginata* among the *Mycena* species available in the GenBank, which possess all-three-loci-sequences. The sizes of DNA sequences of each locus were 645 bp (ITS), 488 bp (RPB1),

and 419 bp (TEF1). We used a total of 1,552 bp sequences following alignment (including gaps). The dataset was aligned using the Muscle algorithm (Edgar, 2004) on the workbench in MEGA v. 7.0.26 software (Kumar et al., 2016). The topology of the maximum likelihood (ML) tree was estimated using RAxML GUI v. 2.0 software (Edler et al., 2021; Stamatakis, 2014). To estimate the optimal base substitution model, Model test v. 3.7 (Posada & Crandall, 1998) was carried out by using PAUP\* 4 (Swofford, 1998), and the GTR+G model was selected as the best one. We assessed the reliability of branching in the tree using nonparametric bootstrap analysis with 1,000 replicates (MLBS). We also estimated the optimal base substitution model to execute Bayesian analysis. MrModeltest v. 2.3 (Nylander, 2008) was carried out using PAUP\* 4 (Swofford, 1998). Following the MrModeltest results, we independently assigned the same substitution model [lset nst = 6, rates = invgamma, and prset statefreqpr = dirichlet (1, 1, 1, 1)] for each locus. We used MrBayes V.3.2.7 software (Ronquist et al., 2012) to construct phylogeny and compute Bayesian inference posterior probability (BPP) for each branch under Bayesian inference. MrBayes analysis involved two sets of four chains of Markov chain Monte Carlo composed of three heated chains and one cold chain, with the topology sampled after every 100 generations. In total, 1,500,000 generations were analyzed until the average standard deviation of the split frequencies was < 0.01. After convergence in the Markov chain Monte Carlo, the first 25% of primary topologies were discarded as burn-in; then the 50% consensus tree was constructed using remaining trees. The tree was visualized using FigTree v.1.4.4 software ([tree.bio.ed.ac.uk/software/figtree/](http://tree.bio.ed.ac.uk/software/figtree/)).

Because only ITS sequences were available for several species of sect. *Calodontes*, we created the ITS phylogenetic tree using *M. rubromarginata* and *M. zephyrus* (Fr.) P. Kumm. as outgroups, similar to Chew et al. (2014). The 79 sequences determined by previous studies (Chew et al., 2014; Cooper, 2018; Harder et al., 2010, 2012, 2013; Liu et al., 2021, 2022; Matheny et al., 2006; Olariaga et al., 2015; Osmundson et al., 2013) and eight sequences identified in our study were analyzed using the GTR+G model and RAxML method (Table 2). In MrBayes analysis, we estimated the optimal base substitution model using KAKUSAN4 (Tanabe, 2011) and GTR+G model was selected. Bayesian analysis was performed using the same method as described previously, except that the dataset was analyzed for 1,000,000 generations.

To conduct species delimitation using genealogical concordance phylogenetic species recognition (GCPsR) (Taylor et al., 2000), we generated independent ITS, TEF1 and RPB1 trees. For molecular phylogenetic analysis of individual regions, we used the same sequences as those used to construct the concatenated three gene tree and the analysis method applied to the concatenated dataset with some minor modifications (Table 2). Briefly, we applied the GTR+G model for ML analysis and the SYM+G model for Bayesian inference in the TEF1 dataset, while the GTR+G model for both was used in the cases of ITS and RPB1. Bayesian analysis was performed for 1,500,000 generations. In the present study, we identified the species boundaries based on the concept of Taylor et al. (2000) that the transition point from concordance to conflict of the tree topologies between separate phylogenetic trees inferred from multiple genetic regions determines the limit of species.

The alignment dataset and resulting trees were deposited in TreeBase (<https://treebase.org/>) under the accession number TB2:S30700 for the tree in Supplementary Fig. S1, TB2:S30701 for Fig. 1, TB2:S31007 for Supplementary Fig. S3 dataset, TB2:S31008 for Supplementary Fig. S4, and TB2:S30699 for Supplementary Fig. S2.





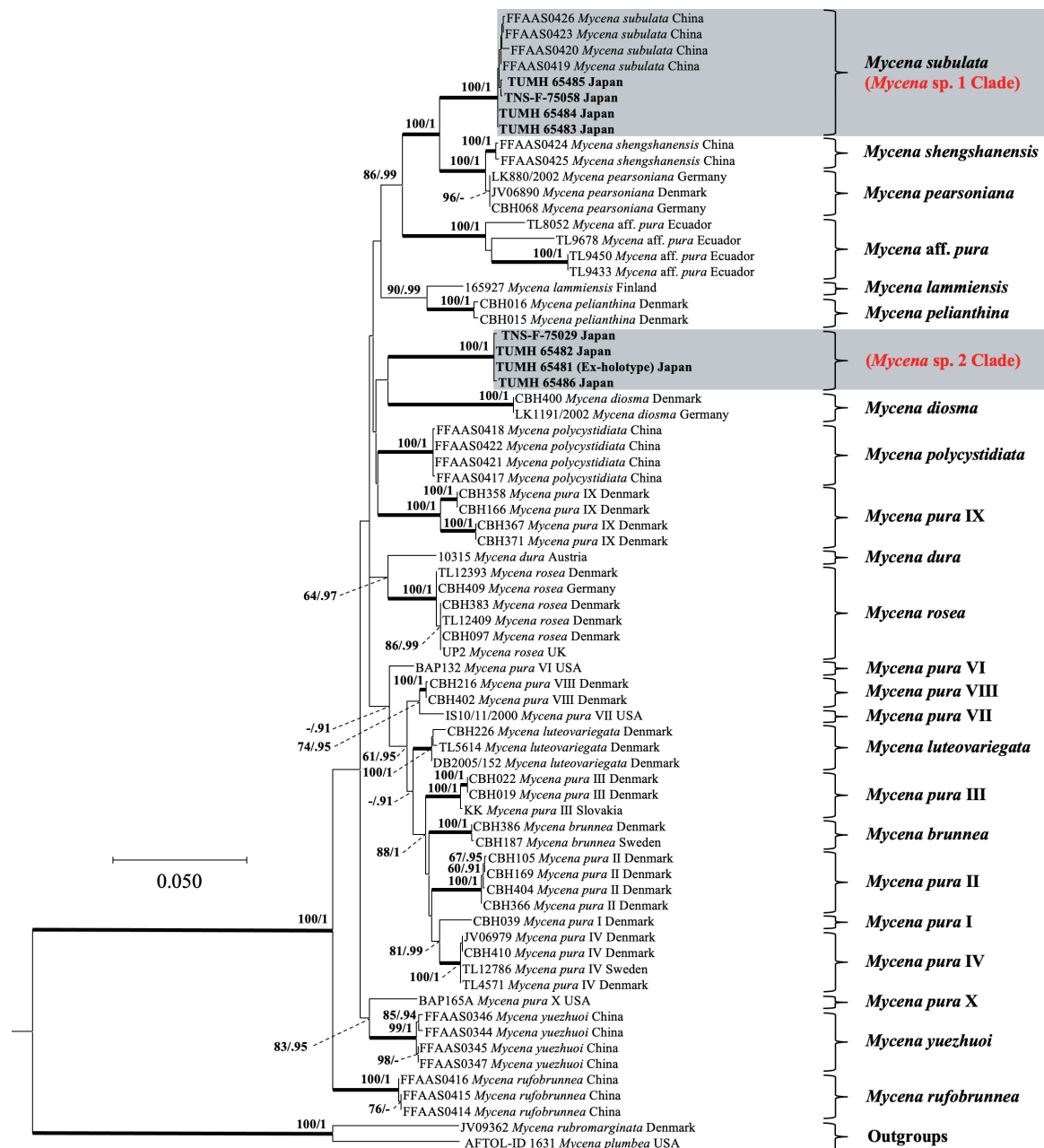


**Fig. 1** – Maximum likelihood (ML) tree of the *Mycena* sect. *Calodontes* inferred from concatenated multigene (ITS, RPBI, TEFI) sequences using RAxML. Statistical supports at the nodes are ML bootstrap support (MLBS)/Bayesian posterior probability (BPP). Thick nodes indicate strong support (MLBS $\geq$ 90 % and BPP $\geq$ 0.95) and omission of the support value shows less than 60 % in MLBS and 0.90 in BPP. Sequences determined in this study are shown in bold letters and the other sequences were obtained from the NCBI database.

### 3. Results

#### 3.1. Morphology

Both “*Mycena* spp.”- 1 and 2 exhibited basidiomata with a reddish tone (pinkish or purplish), smooth cheilocystidia, as well as smooth hyphae of both pileipellis and stipitipellis. These features match the characters of sect. *Calodontes* sensu Maas Geesteranus (1989). “*Mycena* sp.”-1 had inamyloid basidiospores and lacked pleurocystidia corresponding with characteristics of subsect. *Viola-cellae*. This fungus resembles *M. subulata* reported from China (Liu et al., 2022) in having awl-shaped cheilocystidia, but differs from Chinese specimens having amyloid basidiospores. Moreover, Japanese specimens had dextrinoid cheilocystidia and caulocystidia.

“*Mycena* sp.”-2 had amyloid basidiospores and cheilocystidia with a broadly rounded apex, similar to the characteristics of subsect. *Purae* sensu Maas Geesteranus and de Meijer (1997). This fungus had 32–44 lamellae reaching the stipe, bowling-pin shaped cheilocystidia, and amyloid basidiospores, but lacked pleurocystidia. These features are unique among species of sect. *Calodontes*. Morphological comparisons with other phylogenetically related or morphologically similar species are discussed in the “Discussion” part.

#### 3.2. Phylogenetic analyses and species delimitation

Both “*Mycena* spp.”- 1 and 2 formed clades in the position of sect. *Calodontes* in all phylogenetic trees inferred from each of the

ITS, RPB1, and TEF1 sequences and their concatenated data (Fig. 1; Supplementary Figs. S1–S4). “*Mycena* sp.”-1 clustered with Chinese *M. subulata* specimens with high MLBS/BPP values in the concatenated dataset (100/1) and it the individual ITS (98/1), RPB1 (99/1), and TEF1 (100/1) trees. High degrees of DNA homology were observed between Chinese *M. subulata* and Japanese “*Mycena* sp.”-1 specimens (ITS, 97.9–99.8%; RPB1, 98.8–100%; TEF1, 98.2–99.5%). According to the species delimitation using the GCPSR concept, we compared tree topologies at the node connecting eight specimens, including Chinese *M. subulata* and Japanese “*Mycena* sp.”-1. The topologies coincided within ITS, RPB1, and TEF1 phylogenetic trees (= concordance). However, the topologies below that node were different among the trees (= conflict) (Fig. 2; Supplementary Figs. S2–S4). Consequently, *M. subulata* and “*Mycena* sp.”-1 were regarded as conspecific. Although Harder et al. (2013) suggested the possibility of a recombination event occurring in the ITS region in some species of sect. *Calodontes*, no such traces were detected in the multiple alignment of the ITS sequences of Japanese and Chinese *M. subulata* specimens (Supplementary Fig. S5). “*Mycena* sp.”-2 formed a distinct clade clustering without any other species, as indicated by the MLBS/BPP values of 100/1 for the concatenated, 100/1 for ITS, 100/1 for RPB1, and 100/1 for TEF1 trees (Fig. 1; Supplementary Figs. S1–S4). “*Mycena* sp.”-2 formed a sister clade with European *M. diosma* in concatenated and TEF1 trees without MLBS/BPP support (Fig. 1; Supplementary Fig. S3). Topological discordance was observed in the relation between “*Mycena* sp.”-2 and *M. diosma* in ITS and RPB1 trees (Supplementary Figs. S1, S2, S4). In addition, DNA homology between *M. diosma* and “*Mycena* sp.”-2 specimens was 84.1–84.8% in the ITS, 94.3–94.5% in the RPB1, and 89.4% in the TEF1. Therefore, we concluded that “*Mycena* sp.”-2 and *M. diosma* are different species. Although we failed to obtain sequences from Kigawa’s original specimens, the other sequences derived from specimens with similar morphological characteristics to Kigawa’s descriptions (Kigawa, 2017) clustered into the “*Mycena* sp.”-1 or “*Mycena* sp.”-2 clade (Fig. 1; Supplementary Figs. S1–S4). In the three regions where GCPSR were performed, almost all species-clades were reproduced in each tree. However, in the ITS region, *M. luteovariiegata* and *M. pura* IX did not constitute monophyly, which did not match the results of TEF1 and RPB1 trees, as reported by Harder et al. (2013) (Supplementary Figs. S2–S4).

### 3.3. Taxonomy

Based on the phylogenetic and morphological analyses, we con-

cluded that “*Mycena* sp.”-1 is *M. subulata*, which has been described from China, whereas “*Mycena* sp.”-2 is a new species. The morphological characteristics of these species are described below.

***Mycena subulata*** Z.W. Liu, Y.P. Ge & Q. Na, MycoKeys 93: 46 (2022) Fig. 3

Japanese name: Togari-sakura-take (Kigawa, 2017).

**Macromorphology:** Basidiomata (Fig. 3A, B) small- to medium-sized, mycenoid to collybioid. Pileus (Fig. 3C) 15–55 mm in diam, subumbonate to convex; surface light pink (oac487) to brown-pink (oac730); margin striate when wet, gradually disappear as it dry, glabrous, hygrophanous, whitish (oac909) to light pink (oac550) or pale orange (oac682). Pileal context 2 mm in thickness. Lamellae (Fig. 3D, E) 26–33 reaching the stipe, closed to crowded, adnate to subdecurrent, lateral veins and lamellulae are present, light pink (oac549) to pale orange (oac682). Stipe (Fig. 3F) 20–65 mm long, 2–3 mm diam in center, 3–6 mm diam at basal part, smooth, rarely squarrose, light pink (oac550) to pink (oac486) or orange-brown (oac681); base slightly enlarged, tomentose; mycelial cords present or absent, yellow (oac6) to orange (oac811). Odor raphanoid. Taste unknown.

**Micromorphology:** Basidiospores (Fig. 3G, H) 6–7.5(–8) × (4–)4.5(–5.5) μm, Q = (1.32–)1.38–1.70(–1.84), Q<sub>m</sub> = 1.43–1.72 (200 spores from 4 collections), ellipsoid to elongate, rarely pip-shaped, thin-walled, smooth, inamyloid, subhyaline. Basidia (Fig. 3I) (19–)20–24(–26) × (6–)7–8.5 μm, clavate, thin-walled, smooth, inamyloid, 2–4 spored, subhyaline; basal clamps partially present. Sterigmata 1.5–6.5 μm in length, thin-walled, smooth, inamyloid, subhyaline. Basidioles (17.5–)18.5–23(–25) × (5.5–)6–7.5(–8.5) μm, clavate, thin-walled, smooth, inamyloid, subhyaline; basal clamps partially present. Cheilocystidia (Fig. 3J–M) has two shapes; awl-shaped cystidia (33–)39.5–43(–63) × (4.5–)5–8.5(–10.5) μm, thick-walled, smooth, dextrinoid, subhyaline; clavate to obclavate cystidia (26–)27.5–38(–41.5) × (7.5–)8–11.5(–13) μm, thin-walled, smooth, inamyloid, subhyaline; basal clamps partially present. Pleurocystidia absent. Hymenophoral trama subregular, hyphae 2–8 μm regular thin-walled, smooth, dextrinoid, subhyaline; clamp connections partially present. Pileipellis tomentocutis, hyphae 2–6 μm diam, cylindrical, thin-walled, smooth, weakly dextrinoid, subhyaline; clamp connections partially present. Pileocystidia not observed. Pileitrama pseudoparenchymatous, hyphae 9–25 μm diam, cylindrical, thin-walled, smooth, dextrinoid, subhyaline; clamp connections partially present. Stipitipellis parallel, hyphae 2–4 μm diam, cylindrical, smooth, thin-walled, weakly dextrinoid, subhyaline; clamp

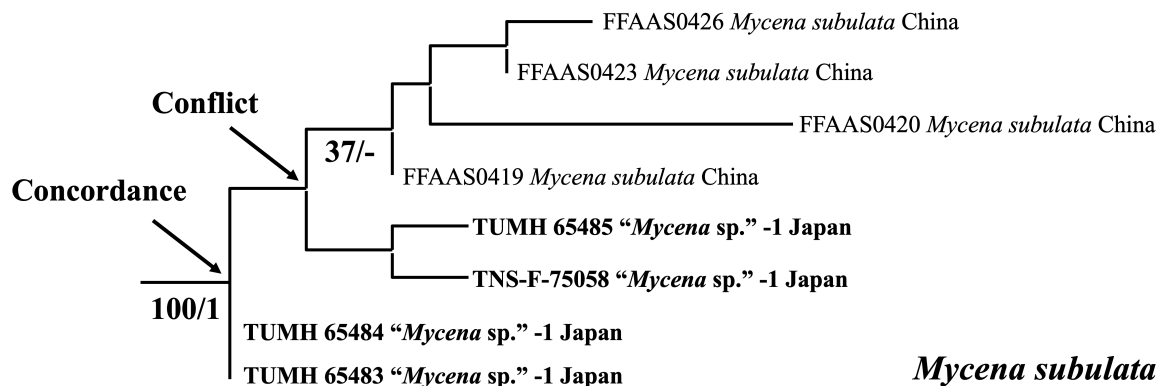


**Fig. 2** – Species delimitation based on the genealogical concordance phylogenetic species recognition (GCPSR) concept. Topology of the three-loci-concatenated tree was employed. “Concordance” shows the node that all three independent trees (ITS, TEF1 and RPB1) corresponded to each other, and “Conflict” shows the node that those independent trees did not correspond to each other. Statistical supports at the nodes are ML bootstrap support (MLBS)/Bayesian posterior probability (BPP). (see also Supplementary Figs. S2–S4).



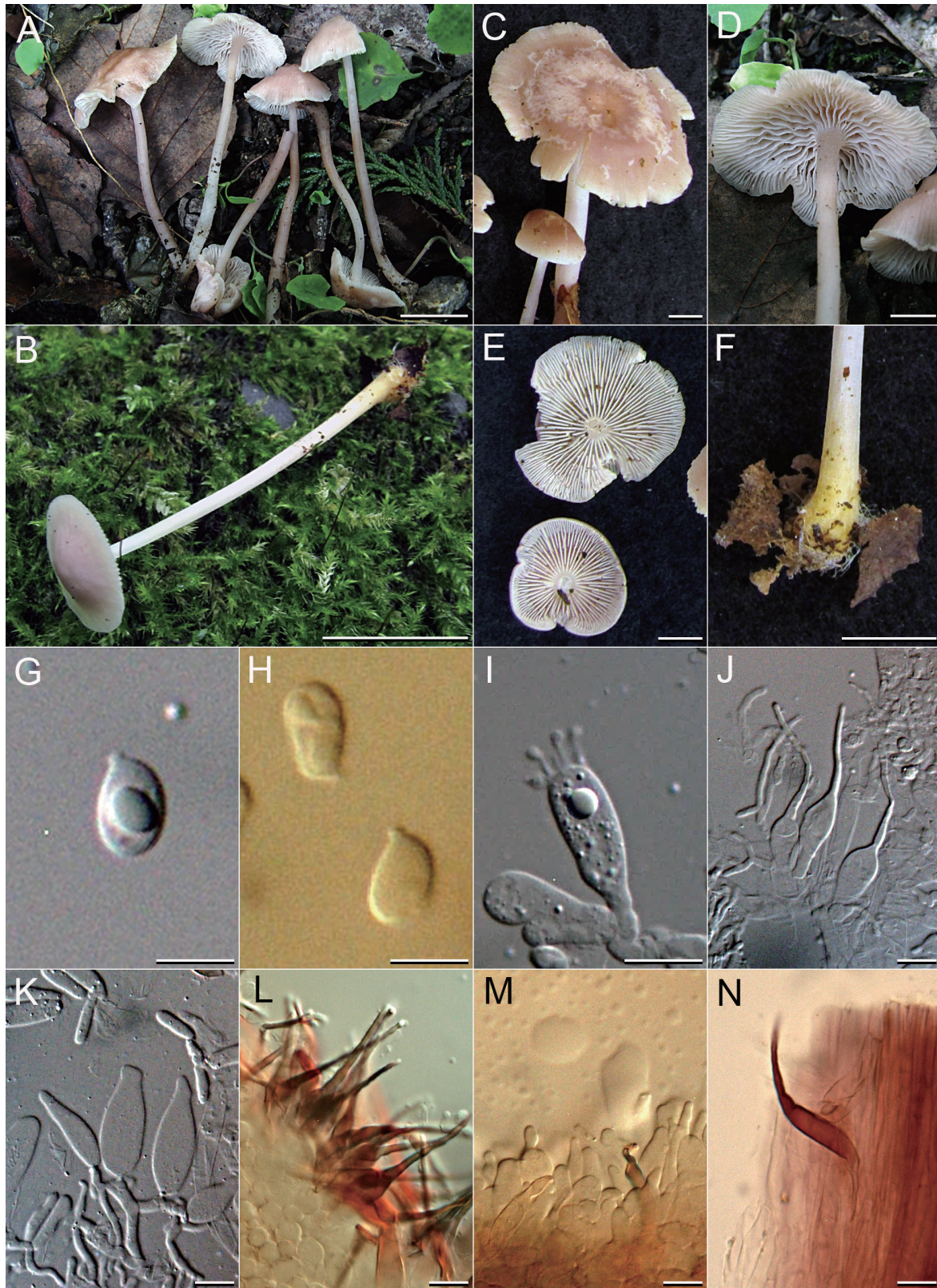


**Fig. 3** – *Mycena subulata*. Macroscopic (A–F) and microscopic (G–N) images. A, B: Basidiomata (A: TUMH 65484; B: TUMH 65483), C: Pileus (TUMH 65485), D, E: Lamellae (D; TUMH 65484, E; TUMH 65485), F: Stipe (TUMH 65483). G: Basidiospore in 3% KOH (TUMH 65484), H: Basidiospores in Melzer's reagent (TUMH 65484), I: Basidium (TUMH 65485), J: awl-shaped cheilocystidia (TUMH 65484), K: Obclavate cheilocystidia (TNS-F-75058), L: awl-shaped cheilocystidia dyeing with Melzer's reagent (TUMH 65483), M: Obclavate cheilocystidia dyeing with Melzer's reagent (TNS-F-75058), N: Caulocystidium dyeing with Melzer's reagent (TUMH 65485). Bars: A, B 15 mm; C–F 5 mm; G, H 5  $\mu$ m; I–N 10  $\mu$ m.



connections partially present. Stipitrama parallel, hyphae 2–13  $\mu\text{m}$  diam, cylindrical to ellipsoid, thin-walled, dextrinoid, subhyaline; clamp connections partially present. Caulocystidia (Fig. 3N) rarely present, 36–60  $\times$  5–9  $\mu\text{m}$ , awl-shaped, thick-walled, smooth, dextrinoid, subhyaline; basal clamps partially present.

Ecology: Cool temperate region of Japan, Sep, solitary to gregarious, on litter layer in *Cryptomeria japonica* (L.f.) D. Don, *Fagus crenata* Blume, *Aesculus turbinata* Blume, and/or *Acer* sp. Heilongjiang Province, China, scattered on the litter layer in *Pinus koraiensis* Siebold et Zucc., *Larix gmelinii* (Rupr.) Rupr. ex Kuzen. and *Tilia* sp. mixed forests.

Materials examined: JAPAN. Tottori Pref., Daisen Town, on the leaf litter in a summer green forest of *Quercus*, 11 Sep 2021, leg. K. Nagamune (Specimen: TUMH 65483; Culture: TUF 102001); Tottori City, Shikano Town, on the ground in a mixed forest of *Acer*, *Chamaecyparis*, *Cerasus*, 19 Sep 2021, leg. K. Nagamune (Specimen: TUMH 65484; Culture: TUF 102002); Kotoura Town, on the ground in a summer green forest of *Fagus*, *Aesculus*, and *Acer*, 20 Sep 2021, leg. R. Sugawara (Specimen: TUMH 65485; Culture: TUF 102003); Saitama Pref., Chichibu City, Nakatsugawa, 28 Sep 2015, leg. K. Hosaka (Specimen: TNS-F-75058); Shizuoka Pref. Gotenba City, 13 Sep 2009, leg. S. Kigawa (Specimen: HCM-58-6665).

Note: Many short and branched spinous seta-like structures were formed on the cultured mycelia (Supplementary Fig. S6). These structures resembled the acanthocytes discovered in the cultured mycelia of *Stropharia rugosoannulata* Farl. ex Murrill as a possible apparatus for defense against nematodes (Yang et al., 2021). A glassy substance covered the seta-like hyphae and could be easily detached and fragmented on slide preparation.

***Mycena densilamellata*** Nagamune, S. Kigawa & N. Endo, sp. nov.

Fig. 4

Mycobank no.: MB 850080

Type: JAPAN, Hokkaido, Ebetsu City, Nopporo Shinrin Kouen Prefectural Natural Park, on the ground of mixed forest where *Picea*, and *Alnus* were dominated, 14 Sep 2019, leg. R. Sugawara (holotype, TUMH 65481; isotype, TNS-F-82703)

Ex-holotype culture: TUF 101999 (polysporic strain)

Gene sequences from ex-holotype culture: LC777686 (ITS), LC777726 (TEF1), LC777734 (RPB1)

Etymology: *densus* (Latin) + *lamellatus* (Latin), referring to the densely formed lamella at the gill of the pileus.

Japanese name: Mitsuhide-sakura-take (Kigawa, 2017).

Macromorphology: Basidiomata (Fig. 4A, B) small- to medium-sized, collybioid. Pileus (Fig. 4C) 20–35 mm in diam, umbonate to subumbonate when young, convex with age; surface purplish (oac427) to dark purplish (oac514); margin striate when wet, gradually disappear as it dries, glabrous, hygrophanous, whitish (oac909) to cream (oac900). Pileal context 2 mm thickness. Lamellae (Fig. 4D, E) 32–44 reaching the stipe, crowded, adnexed to adnate, sub-decurrent, lateral veins and lamellulae present, pale lilac (oac438). Stipe (Fig. 4F) 30–70 mm long, 2–4 mm diam in center, 4–7 mm diam at basal part, smooth or slightly longitudinal striate, pinkish (oac473) to reddish brown (oac525); base slightly enlarged, tomentose, concolorous or yellow (oac6); mycelial cords present or absent, whitish (oac909). Odor raphanoid. Taste unknown.

Micromorphology: Basidiospores (Fig. 4G–I) 5.5–6.5(–7)  $\times$  3–4(–4.5)  $\mu\text{m}$ ,  $Q = (1.50\text{--}1.58\text{--}1.89\text{--}2.02)$ ,  $Q_m = 1.64\text{--}1.80$  (200 spores from 4 collections), ellipsoid to cylindrical, rarely pip-shaped, thin-walled, smooth, amyloid, subhyaline. Basidia (Fig. 4J) (17–)19.5–26(–27.5)  $\times$  (5.5–)6–7(–7.5)  $\mu\text{m}$ , clavate or constricted in

the middle, thin-walled, smooth, inamyloid, subhyaline, 2–4 spored; basal clamps partially present. Sterigmata 1–6  $\mu\text{m}$  length, thin-walled, smooth, inamyloid, subhyaline. Basidiospores (16.5–)18–26(–27.5)  $\times$  (4–)4.5–6.5(–7.5)  $\mu\text{m}$ , clavate, thin-walled, smooth, inamyloid, subhyaline; basal clamps partially present. Cheilocystidia (Fig. 4K–M) (27–)29.5–44(–48)  $\times$  (7–)8–14(–17)  $\mu\text{m}$ , clavate, rarely protruding tip, bowling-pin shaped, thin-walled, smooth, inamyloid, subhyaline; basal clamps partially present. Pleurocystidia absent. Hymenophoral trama subregular, hyphae 3–6  $\mu\text{m}$  diam, thin-walled, smooth, dextrinoid, subhyaline; clamp connections partially present. Pileipellis tomentocutis, hyphae 1–4  $\mu\text{m}$  diam, cylindrical, thin-walled, smooth, inamyloid, subhyaline; clamp connections partially present. Pileocystidia not observed. Pileitrama pseudoparenchymatous, hyphae 4–17  $\mu\text{m}$  diam, cylindrical to ellipsoid, thin-walled, smooth, dextrinoid, subhyaline; clamp connections partially present. Stipitipellis parallel, hyphae 1–2  $\mu\text{m}$  diam, cylindrical, smooth, thin-walled, weakly dextrinoid, subhyaline; clamp connections partially present. Stipitrama parallel, hyphae 3–10  $\mu\text{m}$  diam, cylindrical to slightly expanded, thin-walled, dextrinoid, subhyaline; hyphae, clamp connections partially present. Caulocystidia (Fig. 4N) rarely present, 24–32.5  $\times$  6–8  $\mu\text{m}$ , obclavate to clavate, thin-walled, smooth, inamyloid, subhyaline; basal clamps partially present.

Ecology: Cool temperate region of Japan, Sep to Oct, gregarious to scattered on litter layer in *Quercus serrata* Murray, *Chamaecyparis obtusa* (Siebold et Zucc.) Endl., *Fagus crenata*, *Alnus* sp. *Picea abies* (L.) H. Karst. and *Picea glehnii* (F. Schmidt) Mast.

Other materials examined: JAPAN. Yamanashi Pref., Minamitsuru-gun, Narusawa Village, on the leaf litter in a mixed forest of *Quercus*, *Fagus*, and *Chamaecyparis*, 8 Oct 2020, leg. R. Sugawara (Specimen: TUMH 65486); Tottori Pref., Tottori City, Shikano Town, on the ground in a mixed forest of *Chamaecyparis*, *Quercus*, and *Carpinus*, 19 Sep 2021, leg. K. Nagamune (Specimen: TUMH 65482; Culture: TUF 102000); Saitama Pref., Chichibu City, Nakatsugawa, 28 Sep 2015, leg. K. Hosaka (Specimen: TNS-F-75029); Shizuoka Pref. Gotenba City, 13 Sep 2009, leg. S. Kigawa (Specimen: HCM-58-6667).

Note: Many short and branched acanthocyte-like structures were formed on the cultured mycelia (Supplementary Fig. S7) as observed in “*Mycena* sp.”-1 cultures (see above).

#### 4. Discussion

“*Mycena* sp.”-1 constituted a clade with the Chinese specimens of *M. subulata* (Fig. 1; Supplementary Figs. S1–S4) and showed similar characteristics of narrowly fusiform, long, and narrow protruberance of cheilocystidia (Fig. 3). The delimitation of species according to the GCPSR concept (Fig. 2) strongly suggested conspecificity. *Mycena subulata* has not been reported previously from Japan. Here, we assign the Japanese name “*Togari-sakura-take*”, to the species, consistent with Kigawa (2017). However, our specimens from Japan did not show the amyloid basidiospores, which differed from the original description by Liu et al. (2022). Although the Japanese specimens showed dextrinoid cheilocystidia, Liu et al. (2022) did not include this characteristic in the original description. It is necessary to observe more specimens (including the type specimen) to determine whether these features exhibit regional differences among the Japanese samples. In the detailed analysis of the molecular data, seven mutation sites in the ITS were detected between Chinese and Japanese *M. subulata* (Supplementary Fig. S5). However, these base differences did not distinguish between Chinese and Japanese specimens on the phylogenetic trees (Supplementary Figs. S1, S2).



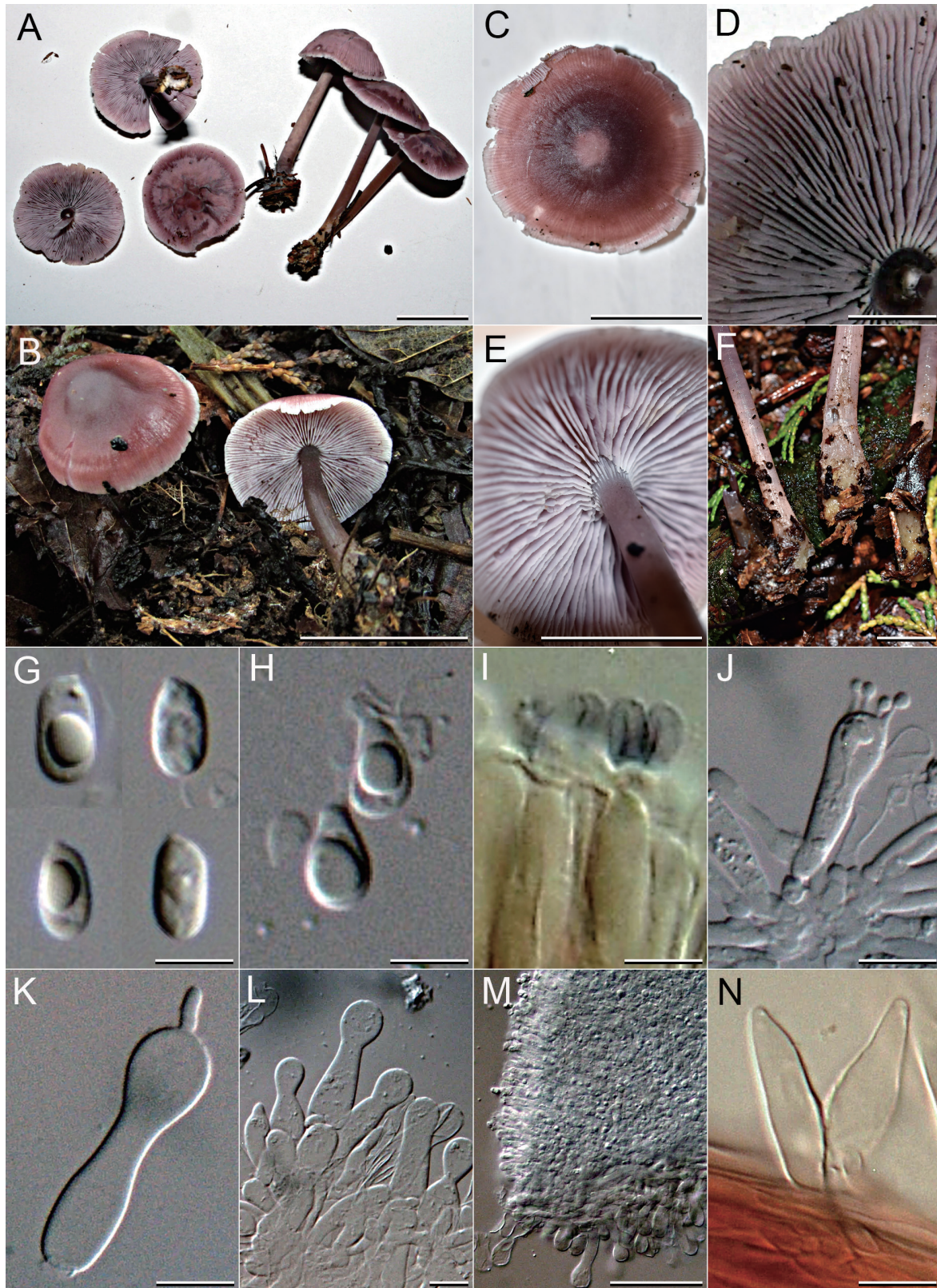


**Fig. 4** – *Mycena densilamellata*. Macroscopic (A–F) and microscopic (G–N) images. A, B: Basidiomata (A: TUMH 65481, holotype; B: TUMH 65482), C: Pileus (TUMH 65486), D: Lamellae (TUMH 65482), E: Decurrent lamellae (TUMH 65486), F: Stipes (TUMH 65486). G: Basidiospores (TUMH 65481), H: Pip-shaped basidiospores (TUMH 654826), I: Basidiospores dyeing with Melzer's reagent (TUMH 65481), J: Basidium (TNS-F-75029), K: Cheilocystidium with protruding tip (TUMH 65481). L: Clavate and bowling-pin shaped cheilocystidia (TUMH 65486), M: Hymenium and lamellar edge (TUMH 65482), N: Caulocystidia in Melzer's reagent (TUMH 65486). Bars: A, B 20 mm; C, E 10 mm; D, F 5 mm; G–I 5  $\mu$ m; J–L, N 10  $\mu$ m; M 50  $\mu$ m.



Liu et al. (2022) did not specify the subsection of *M. subulata* based on the amyloid basidiospores and lack of pleurocystidia. On the other hand, all five of our Japanese specimens demonstrated inamyloid basidiospores, indicating their similarity to the species of subsect. *Violacellae*. Harder et al. (2012) suggested the phylogenetic position of subsect. *Violacellae* in the ITS region by designating the epitype of *M. pearsoniana* Dennis ex Singer. *Mycena subulata* showed a phylogenetic position close to *M. pearsoniana* (Liu et al., 2022); our results support that (Fig. 1). Moreover, *M. pearsoniana* has inamyloid to weakly amyloid basidiospores, suggesting that amyloidity is not a diagnostic feature of species in *M. pearsoniana* (Harder et al., 2012). *Mycena subulata* and *M. pearsoniana* form a highly supported clade (MLBS/BPP = 96/1), which includes the *M. shengshanensis* described by Liu et al. (2022); a similar pattern was also found in the present study (MLBS/BPP = 100/1) (Fig. 1). *Mycena subulata* possesses both inamyloid and weakly amyloid basidiospores within the species as *M. pearsoniana*. Based on these results, we propose that *M. subulata* should be assigned to subsect. *Violacellae*. Although the morphological characteristics of subsect. *Generosae* coincide with those of *M. subulata* described by Liu et al. (2022), the phylogenetic position of subsect. *Generosae* has not been clarified. Hence, it is necessary to investigate the phylogenetic position of *M. generosa*, the type species of subsect. *Generosae* and the phylogenetic relationship between this subsection and *M. subulata*.

We assigned the Japanese name “*Mitsuhide-sakura-take*” to *M. densilamellata* consistent with Kigawa (2017). This species differs from other species in sect. *Calodontes* based on the formation of close lamellae, lack of pleurocystidia, and presence of bowling pin-shaped cheilocystidia and amyloid basidiospores. A few specimens had protruding tips of cheilocystidia, the most of which had broadly rounded apices (Fig. 4). These characteristics indicate that *M. densilamellata* belongs to subsect. *Purae* according to the definition by Maas Geesteranus and de Meijer (1997). *Mycena diosma* Krieglst. & Schwöbel from the subsect. *Purae* resembles *M. densilamellata* in terms of its pileus color (Harder et al., 2010; Krieglsteiner & Schwöbel, 1982). Despite the lack of significant statistical support and topological incongruence between datasets, our three-loci-concatenated and TEF1 trees suggested a potential sister relationship between the two species (Fig. 1; Supplementary Fig. S3). *Mycena diosma* has close lamellae (with 24–32 reaching the stipe) (Krieglsteiner & Schwöbel, 1982), whereas *M. densilamellata* exhibits crowding (with 32–44 reaching the stipe). In addition, *M. diosma* has few to no pleurocystidia depending on the specimen (Harder et al., 2010; Krieglsteiner & Schwöbel, 1982), whereas pleurocystidia are entirely lacking in *M. densilamellata*. *Mycena densilamellata* resembles *M. yuezhuoi* in terms of amyloid basidiospores and lack of pleurocystidia. However, *M. yuezhuoi* has slightly closer lamellae (with 21–26 reaching the stipe) emarginated to a stipe (Liu et al., 2021), whereas *M. densilamellata* exhibits crowded, adnate to decurrent lamellae (with 32–44 reaching the stipe). Furthermore, these two species are categorized in different clades according to the phylogenetic analysis (Fig. 1; Supplementary Figs. S1–S4). *Mycena kuehneriana* A.H. Sm. resembles *M. densilamellata* in terms of its amyloid basidiospores and lack of pleurocystidia. However, *M. kuehneriana* has subfusoid to nearly cylindrical cheilocystidia and scattered to rare cheilocystidia (Smith, 1947). *Mycena densilamellata* is distinguishable from *M. kuehneriana* by its abundant bowling pin-shaped cheilocystidia. According to Maas Geesteranus (1989), 20 lamellae of *M. kuehneriana* reached the stipe, with scattered pleurocystidia, whereas *M. densilamellata* produced 32–44 stipe-reaching lamella without pleurocystidia. Although the crowding of lamellae is a characteristic feature of *M. densilamella-*

*ta*, *M. rosea*, *M. sororia* Perr.-Bertr., Boissel. & Lambourd. and *M. vinacea* Cleland also have similar characteristics [with 40, 38–42, and 32–40 lamellae reaching the stipe, respectively (Grgurinovic, 1997; Maas Geesteranus, 1989; Perreau-Bertrand et al., 1996)]. However, *M. densilamellata* lacks pleurocystidia, whereas the other three have pleurocystidia. In addition, *M. densilamellata* is distinguishable from the other three based on cheilocystidia shape: those of *M. densilamellata* are bowling pin-shape, whereas they are fusiform, clavate, or subcylindrical in *M. rosea* (Maas Geesteranus, 1989); clavate, subcylindrical, or fusiform in *M. sororia* (Perreau-Bertrand et al., 1996); and cylindrical, cylindro-ventricose, or clavate in *M. vinacea* (Grgurinovic, 1997). Further detailed comparisons with species, including the remaining sect. *Calodontes* species, are presented in Supplementary Table S1. The original description of *M. sororia* is available, but the lack of type specimen and molecular information make it difficult to verify the taxonomic status of this species (Harder et al., 2010). For future revision of the whole sect. *Calodontes* species, there is an urgent need to redesignate the type specimen to allow molecular phylogenetic analyses of such species.

According to Chew et al. (2014) and Harder et al. (2012), the species of subsect. *Marginatae* and subsect. *Violacellae* formed independent monophyly, whereas those of subsect. *Purae* were separated into multiple clades. The phylogenetic trees constructed by Liu et al. (2021, 2022) based on the three loci (ITS, TEF1, and RPB1) exhibited polyphyly of subsect. *Purae*. In our phylogeny based on the three loci, monophyly of subsect. *Marginatae* was observed; however, subsect. *Purae* was also polyphyletic. *M. pearsoniana* and *M. subulata* had a similar morphological appearance to subsect. *Violacellae*, forming a robust monophyletic clade. However, *M. shengshanensis*, which cannot be assigned to any subsection due to its morphological characteristics (Liu et al., 2022), occupies an intermediate position between *M. pearsoniana* and *M. subulata* (Fig. 1), thereby necessitating the revision of subsect. *Violacellae* after consideration of the accuracy of the morphological description of *M. shengshanensis* by Liu et al. (2022). However, we found potential inaccuracies in the original description of *M. subulata*.

Currently, there is insufficient DNA data to determine the phylogenetic relationships among infrageneric taxa. To date, ITS sequences of 20 species belonging to sect. *Calodontes* have been registered in the GenBank database, which is < 50% of the known species. Among them, only 15 species, including the novel species, have records of authentic sequences obtained from the type materials. (Chew et al., 2014; Cooper, 2018; Harder et al., 2012, 2013; Liu et al. 2021, 2022; Olariaga et al., 2015). Moreover, the number of available sequences of TEF1 and RPB1 genes is even more limited (Harder et al., 2013; Liu et al., 2021, 2022). The phylogenetic position of subsection *Generosae* has not been confirmed. Thus, the unavailability of DNA information makes it challenging to determine whether or not the characteristic morphological features of each subsection reflect their phyletic relationship. Harder et al. (2013) suggested that TEF1 may be a more reliable marker for species identification in sect. *Calodontes* compared to ITS and RPB1. Indeed, only TEF1 indicated potential separation between the Japanese and Chinese populations of *M. subulata*, although this lacked statistical support (Supplementary Figs. S2–S4). In addition, TEF1 alone suggested a potential sister group relation between *M. densilamellata* and *M. diosma*, but this association also lacked statistical support (Supplementary Fig. S3). In future studies, it will be necessary to collect specimens from various parts of the world and obtain additional DNA sequences. This should include not only ITS, TEF1, and RPB1, but also other frequently used regions, such as RPB2, ATP6, etc., along with morphological characteristics.

These combined efforts will contribute to the construction of a robust infrageneric classification system accurately reflecting the phylogenetic relations and help to determine the most effective DNA marker for species identification in sect. *Calodontes*.

The fruiting bodies of *M. subulata* and *M. densilamellata* predominantly emerged on litter within the broadleaved forests dominated by oak and beech trees at altitudes exceeding 450 m above sea level across the Japanese mainland. Specimens of *M. subulata* were collected from Eastern (Saitama Pref.) and Western (Tottori Pref.) regions of Japan. Similarly, specimens of *M. densilamellata* were collected from Northern (Hokkaido) and Western (Tottori Pref.) regions of Japan. Thus, both species are widely distributed in broadleaved forests in Japan. *Mycena* species in sect. *Calodontes* have been well described in Europe since the mid-18th century, whereas few taxonomic studies have been conducted in Asia (Aravindakshan & Manimohan, 2015; Chew et al., 2014; Hennings 1900; Liu et al., 2021, 2022). Further studies on the taxonomy and ecology of *Mycena* species in Asia are required to gain a thorough understanding of the distribution of these species. On the cultured mycelia of *M. subulata* and *M. densilamellata*, we observed acanthocyte-like structures similar to those described by Yang et al. (2021) (Supplementary Figs. S6, S7). On the other hand, Chew et al. (2014) reported inamyloid crystals on mycelia of *M. cahaya* cultured on MEA. Because we could not verify whether the acanthocyte-like structures covered with glassy substance found in the two *Mycena* species are identical with one of the previously reported structures, further studies are required to observe their detailed structure and development process. It is also essential to consider their taxonomic importance and ecological function by culture studies of various fungal species of sect. *Calodontes*.

## Disclosure

The authors have no conflicts of interest to declare. All experiments undertaken in this study complied with the current laws of the country where they were performed.

## Acknowledgements

We thank Noriko Matsumoto, a curator at the Hiratsuka City Museum, for loaning the specimens of “*Mitsuhide-sakura-take*” and “*Togari-sakura-take*”, and Kanagawa mushroom club’s members, who collected these samples. We also thank Yamanashi Prefectural Government for generously allowing the sampling of *Mycena* within the forests of Narusawa Village, Yamanashi Prefecture, Japan; and thank to Hiroko Shirayama and Seiichi Takeda for helping collect these samples; and Eiji Nagasawa to provide information regarding *Mycena rosea*; and Shuji Ushijima to help literature searching. This work was partially supported by JSPS KAKEN-HI (grant nos.: 20K06805 and 24680085).

## References

Aravindakshan, D. M., & Manimohan, P. (2015) *Mycenas of Kerala*. SporePrint Books. <http://dx.doi.org/10.13140/RG.2.1.2116.4003>

Binder, M., Larsson, K. H., Matheny, P. B., & Hibbett, D. S. (2010). *Amylocorticiales* ord. nov. and *Jaapiales* ord. nov.: early diverging clades of *Agaricomycetidae* dominated by corticioid forms. *Mycologia*, 102, 865–880. <https://doi.org/10.3852/09-288>

Cha, J. Y., Lee, S. Y., Chun, K. W., Lee, S. Y., & Ohga, S. (2010). A new record of a snowbank fungus, *Mycena overholtsii*, from Japan. *Journal of the Faculty of Agriculture, Kyushu University*, 55, 77–78. <https://doi.org/10.5109/17804>

Chew, A. L., Tan, Y. S., Desjardin, D. E., Musa, M. Y., & Sabaratnam, V. (2014). Four new bioluminescent taxa of *Mycena* sect. *Calodontes* from Peninsular Malaysia. *Mycologia*, 106, 976–988. <https://doi.org/10.3852/13-274>

Cooper, A. C. (2018). *A taxonomic investigation of Mycena of Sao Tome and Principe* (Master Thesis). San Francisco State University.

Davey, M. L., Heimdal, R., Ohlson, M., & Kausrud, H. (2013). Host-and tissue-specificity of moss-associated *Galerina* and *Mycena* determined from amplicon pyrosequencing data. *Fungal Ecology*, 6, 179–186. <https://doi.org/10.1016/j.funeco.2013.02.003>

Edgar, R. C. (2004). Muscle: Multiple sequence alignment with high accuracy and high throughput. *Nucleic Acids Research*, 32, 1792–1797. <https://doi.org/10.1093/nar/gkh340>

Edler, D., Klein, J., Antonelli, A., & Silvestro, D. (2021). raxmlGUI 2.0: a graphical interface and toolkit for phylogenetic analyses using RAxML. *Methods in Ecology and Evolution*, 12, 373–377. <http://doi.org/10.1111/2041-210X.13512>

Gardes, M., & Bruns, T. D. (1993). ITS primers with enhanced specificity for basidiomycetes-application to the identification of mycorrhizae and rusts. *Molecular Ecology*, 2, 113–118. <https://doi.org/10.1111/j.1365-294X.1993.tb00005.x>

Grgurinovic, C. A. (1997). *The genus Mycena in south-eastern Australia: a taxonomic, phylogenetic and bioclimatic study of some sections* (PhD Thesis). The University of New South Wales, Sydney. <https://doi.org/10.26190/unsworks/7165>

Hall, T. A. (1999). BioEdit: A user-friendly biological sequence alignment editor and analysis program for Windows 95/98/NT. *Nucleic Acids Symposium Series*, 41, 95–98.

Harder, C. B., Hesling, E., Botnen, S. S., Lorberau, K. E., Dima, B., von Bonsdorff-Salminen, T., Niskanen, T., Jarvis, S. G., Oimette, A., Hester, A., Hobbie, E. A., Taylor, A. F. S., & Kausrud, H. (2023). *Mycena* species can be opportunistic generalist plant root invaders. *Environmental Microbiology*, 25, 1875–1893. <https://doi.org/10.1111/1462-2920.16398>

Harder, C. B., Læssøe, T., Frøslev, T. G., Ekelund, F., Rosendahl, S., & Kjoller, R. (2013). A three-gene phylogeny of the *Mycena pura* complex reveals 11 phylogenetic species and shows ITS to be unreliable for species identification. *Fungal Biology*, 117, 764–775. <https://doi.org/10.1016/j.funbio.2013.09.004>

Harder, C. B., Læssøe, T., Kjoller, R., & Frøslev, T. G. (2010). A comparison between ITS phylogenetic relationships and morphological species recognition within *Mycena* sect. *Calodontes* in Northern Europe. *Mycological Progress*, 9, 395–405. <https://doi.org/10.1007/s11557-009-0648-7>

Harder, C. B., Lodge, D. J., Petersen, R. H., Hughes, K. W., Blanco, J. C., Frøslev, T. G., & Læssøe, T. (2012). Amyloidity is not diagnostic for species in the *Mycena pearsoniana* complex (*Mycena* sectio *Calodontes*). *Mycological Progress*, 11, 725–732. <https://doi.org/10.1007/s11557-011-0782-x>

He, M. Q., Zhao, R. L., Hyde, K. D., Begerow, D., Kemler, M., Yurkov, A., McKenzie, E. H. C., Raspé, O., Kakishima, M., Sánchez-Ramírez, S., ... & Kirk, P. M. (2019). Notes, outline and divergence times of Basidiomycota. *Fungal Diversity*, 99, 105–367. <https://doi.org/10.1007/s13225-019-00435-4>

Hennings, P. (1900). Fungi. II. In: O. Warburg (Ed.), *Monsunia: Beiträge zur Kenntnis der Vegetation des süd-und ostasiatischen Monsungebietes* (pp. 137–174). Verlag von Wilhelm Engelmann.

Hongo, T. (1953). Larger fungi of the provinces of Omi and Yamashiro (5). *Journal of Japanese Botany*, 28, 330–336.

Hosaka, K., & Nam, K.-O. (2023) Polymerase chain reaction with a reduced ramp rate: a case study from fungal *atp6*. *Bulletin of the National Museum of Nature and Science, Series B*, 49, 41–48. [https://doi.org/10.50826/bnmnsbot.49.2\\_41](https://doi.org/10.50826/bnmnsbot.49.2_41)

Imai, S. (1938). Studies on the Agaricaceae of Hokkaido. I. Hokkaido Imperial University *Journal of the Faculty of Agriculture*, 43, 1–178.

Izumitsu, K., Hatoh, K., Sumita, T., Kitade, Y., Morita, A., Gafur, A., Ohta, A., Kawai, M., Yamanaka, T., Neda, H., Ota, Y., & Tanaka, C. (2012). Rapid and simple preparation of mushroom DNA directly from colonies and fruiting bodies for PCR. *Mycoscience*, 53, 396–401. <https://doi.org/10.1007/s10267-012-0182-3>

Katsumoto, K. (2010). *List of fungi recorded in Japan* [in Japanese]. The Kanto Branch of the Mycological Society of Japan.

Kausrud, H., & Schumacher, T. (2001). Outcrossing or inbreeding: DNA markers provide evidence for type of reproductive mode in *Phellinus nigrolimitatus* (Basidiomycota). *Mycological Research*, 105, 676–683. <https://doi.org/10.1017/S0953756201004191>

Kigawa, S. (2017). *Kenushou-kinoko-shinn-zukan* [New Illustrated Book of Mushrooms for Verification, in Japanese]. Tsukuba-shobo.

Kitahara, M., Nagamune, K., Kinoshita, A., Yugeta, C., Ohara, N., Shimazaki, A., Yamashita, Y., Yukawa, T., Endo N., & Ogura-Tsujita, Y. (2022). In-vitro symbiotic germination of seeds of five mycoheterotrophic *Gastrodia* orchids with *Mycena* and *Marasmiaceae* fungi. *Mycoscience*, 63, 88–95. <https://doi.org/10.47371/mycosci.2022.04.001>

Kramer, L. A. (2004). *The Online Auction Color Chart*. The Online Auction Color Chart Company, Stanford.

Kriegelsteiner, G. J., & Schwöbel, H. (1982). *Mycena diosma* spec. nov. und der *Mycena-pura*-Formkreis in Mitteleuropa. *Zeitschrift Fur Mykologie*, 48, 25–34.

Krishnan, S. (2017). Sustainable coffee production. In: *Oxford research encyclopedia*



- of environmental science. <https://doi.org/10.1093/acrefore/9780199389414.013.224>
- Kudo, S., & Nagasawa, E. (2009). *Tohoku-kinoko-zukan* [Illustrated Book of Mushroom rooms in Tohoku region, in Japanese]. Ie-no-hikari-kyokai.
- Kudo, S., & Nagasawa, E. (2017). *Macrofungi of Aomori* [in Japanese]. Akuse-su-21-syuppan.
- Kumar, S., Stecher, G., & Tamura, K. (2016). MEGA7: Molecular Evolutionary Genetics Analysis Version 7.0 for Bigger Datasets. *Molecular Biology and Evolution*, *33*, 1870–1874. <https://doi.org/10.1093/molbev/msw054>
- Liu, Z., Ge, Y., Zeng, H., Cheng, X., & Na, Q. (2022). Four new species of *Mycena* sect. *Calodontes* (Agaricales, Mycenaceae) from northeast China. *MycKeys*, *93*, 23–56. <https://doi.org/10.3897/mycokeys.93.86580>
- Liu, Z., Na, Q., Cheng, X., Wu, X., & Ge, Y. (2021). *Mycena yuezhuo* sp. nov. (Mycenaceae, Agaricales), a purple species from the peninsula areas of China. *Phytotaxa*, *511*, 148–162. <https://doi.org/10.11646/phytotaxa.511.2.3>
- Maas Geesteranus, R. A. (1980). Studies in Mycenaceae—15. A tentative subdivision of the genus *Mycena* in the northern Hemisphere. *Persoonia-Molecular Phylogeny and Evolution of Fungi*, *11*, 93–120.
- Maas Geesteranus, R. A. (1989). Conspectus of the Mycenaceae of the Northern Hemisphere-13. Sections *Calamophilae* and *Calodontes*. *Proceedings of the Koninklijke Nederlandse Akademie van Wetenschappen: Series C: Biological and medical sciences*, *92*, 477–504.
- Maas Geesteranus, R. A., de Meijer AAR (1997) *Mycenae Paranaenses*. North-Holland.
- Matheny, P. B., Curtis, J. M., Hofstetter, V., Aime, M. C., Moncalvo, J. M., Ge, Z. W., Slot, J. C., Ammirati, J. F., Baroni, T. J., Bougher, N. L., Hughes, K. W., Lodge, D. J., Kerrigan, R. W., Seidl, M. T., Aanen, D. K., DeNitis, M., Daniele, G. M., Desjardin, D. E., Kropp, B. R., ... Hibbett, D. S. (2006). Major clades of Agaricales: a multilocus phylogenetic overview. *Mycologia*, *98*, 982–995. <https://doi.org/10.1080/15572536.2006.11832627>
- Murata, Y. (1979). New records of gill fungi from Hokkaido [in Japanese], 3. *Transactions of the Mycological Society of Japan*, *20*, 125–131.
- Nylander, J. A. A., 2008. MrModeltest v2.3. Program distributed by the author. Evolutionary Biology Centre, Uppsala University. <http://www.abc.se/wnylander/mrmodeltest2/mrmodeltest2.html>. Accessed Apr 2013.
- Olariaga, I., Pérez-de-Gregorio, M. À., & Arrillaga, P. (2015). *Porpoloma aranzadii* is a synonym of *Mycena dura* further notes in *Mycena* sect. *Calodontes*. *Cryptogamie, Mycologie*, *36*, 253–264. <https://doi.org/10.7872/crym/v36.iss3.2015.253>
- Osmundson, T. W., Robert, V. A., Schoch, C. L., Baker, L. J., Smith, A., Robich, G., & Garbelotto, M. M. (2013). Filling gaps in biodiversity knowledge for macrofungi: contributions and assessment of an herbarium collection DNA barcode sequencing project. *PLoS ONE*, *8*, e62419.
- Perreau-Bertrand, J., Boisselier-Dubayle, M. C., & Lambourdiere, J. (1996). *Mycena sororia* sp. nov., close to *M. rosea* Gramberg (*Basidiomycotina*). *Mycotaxon*, *60*, 263–273.
- Posada, D., & Crandall, K. A. (1998). MODELTEST: testing the model of DNA substitution. *Bioinformatics*, *14*, 817–818. <https://doi.org/10.1093/bioinformatics/14.9.817>
- Rehner, S. A., & Buckley, E. (2005). A *Beauveria* phylogeny inferred from nuclear ITS and EF1- $\alpha$  sequences: evidence for cryptic diversification and links to *Cordyceps* teleomorphs. *Mycologia*, *97*, 84–98. <https://doi.org/10.1080/15572536.2006.11832842>
- Ronquist, F., Teslenko, M., van der Mark, P., Ayres, D. L., Darling, A., Höhna, S., & Huelsenbeck, J. P. (2012). MrBayes 3.2: efficient Bayesian phylogenetic inference and model choice across a large model space. *Systematic Biology*, *61*, 539–542. <https://doi.org/10.1093/sysbio/sys029>
- Shirayama, H. (2010). *Mycena aurantiomarginata* newly recorded from Japan. *Nippon Kingakukai Kaiho*, *51*, 22–25.
- Smith, A. H. (1947) *North American species of Mycena*. University of Michigan Press.
- Stamatakis, A. (2014). RAxML version 8: a tool for phylogenetic analysis and post-analysis of large phylogenies. *Bioinformatics*, *30*, 1312–1313. <https://doi.org/10.1093/bioinformatics/btu033>
- Swofford, D. L. (1998). PAUP\*. Phylogenetic Analyses Using Parsimony (\*And Other Methods)
- Tanabe, A. S. (2011). Kakusan4 and Aminosan: two programs for comparing non-partitioned, proportional and separate models for combined molecular phylogenetic analyses of multilocus sequence data. *Molecular Ecology Resources*, *11*, 914–921. <https://doi.org/10.1111/j.1755-0998.2011.03021.x>
- Taylor, J. W., Jacobson, D. J., Kroken, S., Kasuga, T., Geiser, D. M., Hibbett, D. S., & Fisher, M. C. (2000). Phylogenetic species recognition and species concepts in fungi. *Fungal Genetics and Biology*, *31*, 21–32. <https://doi.org/10.1006/fgbi.2000.1228>
- Terashima, Y., Takahashi, H., & Taneyama, Y. (2016) *The fungal flora in southwestern Japan: Agarics and boletes* [in Japanese]. Tokai University Press.
- Thoen, E., Harder, C. B., Kausrud, H., Botnen, S. S., Vik, U., Taylor, A. F. S., Menkis, A., & Skrede, I. (2020). In vitro evidence of root colonization suggests ecological versatility in the genus *Mycena*. *New Phytologist*, *227*, 601–612. <https://doi.org/10.1111/nph.16545>
- Vilgalys, R., & Hester, M. (1990). Rapid genetic identification and mapping of enzymatically amplified ribosomal DNA from several *Cryptococcus* species. *Journal of Bacteriology*, *172*, 4238–4246. <https://doi.org/10.1128/jb.172.8.4238-4246.1990>
- White, T. J., Bruns, T., Lee, S. J. W. T., & Taylor, J. (1990). Amplification and direct sequencing of fungal ribosomal RNA genes for phylogenetics. In: M. A. Innis, D. H. Gelfand, J. J. Sninsky, & T. J. White (Eds.), *PCR protocols: a guide to methods and applications* (pp. 315–322). Academic Press.
- Wijayawardene, N. N., Hyde, K. D., Al-Ani, L. K. T., Tedersoo, L., Haelewaters, D., Rajeshkumar, K. C., Zhao, R. L., Aptroot, A., Leontyev, D. V., Saxena, R. K., Tokarev, Y. S., Dai, D. Q., Letcher, P. M., Stephenson, S. L., Ertz, D., Lumbsch, H. T., Kukwa, M., Issi, I. V., Madrid, H., ... Thines, M. (2020). Outline of Fungi and fungus-like taxa. *Mycosphere*, *11*, 1060–1456. <https://doi.org/10.5943/mycosphere/11/1/8>
- Yang, Y., Li, C., Ni, S., Zhang, H., & Dong, C. (2021). Ultrastructure and development of acanthocytes, specialized cells in *Stropharia rugosoannulata*, revealed by scanning electron microscopy (SEM) and cryo-SEM. *Mycologia*, *113*, 65–77. <https://doi.org/10.1080/00275514.2020.1823184>